JOURNAL OF SPACECRAFT AND ROCKETS
Vol. 42, No. 2, March–April 2005

Cost–Benefit Analysis of the Aerocapture Mission Set

Jeffery L. Hall,* Muriel A. Noca,† and Robert W. Bailey‡
Jet Propulsion Laboratory, California Institute of Technology, Pasadena, California 91109

Calculations have been performed to quantify the cost and delivered mass advantages of aerocapture at all destinations in the solar system with significant atmospheres. A total of 11 representative missions were defined for the eight possible destinations and complete launch-to-orbit insertion architectures constructed based on available U.S. launch vehicles. Direct comparisons were made between aerocapture and competing orbit insertion techniques based on state-of-the-art and advanced chemical propulsion, solar electric propulsion, and aerobraking. The results show that three of the missions cannot be done without aerocapture: delivery of spacecraft into elliptical orbits at Neptune and circular orbits at Jupiter or Saturn. Aerocapture was found to significantly enhance five other missions by putting larger, and usually very much larger, spacecraft into the target orbit for approximately the same overall delivery cost as the best nonaerocapture alternative: delivery of spacecraft into Venus circular orbits (79% more mass), Venus elliptical orbits (43%), Mars circular orbits (15%), Titan circular orbits (280%), and Uranus elliptical orbits (218%). These results, and other delivery cost per unit delivered mass metrics, were found to be not very sensitive to 30% increases in both the estimated aerocapture system mass and system cost, suggesting that even modestly performing aerocapture systems will yield substantial mission benefits. Two other missions consisting of spacecraft inserted into high-eccentricity elliptical orbits at Mars and Jupiter were shown to be not improved by aerocapture. The last mission in the set consisting of an aeroassisted orbit transfer at Earth showed that aerocapture technology offered a 32% $/kg reduction compared to chemical propulsion, but that aerobraking offered even better performance. Nevertheless, the problems of repeated passes through the Van Allen radiation belts are likely to preclude Earth aerobraking for most applications.

Nomenclature

C_3 = square of the hyperbolic excess velocity, km^2/s^2
g_0 = gravitational constant, 9.81 m/s^2
I_{sp} = propulsion system specific impulse, s
m_f = final (postmaneuver) spacecraft mass, kg
m_i = initial (premaneuver) spacecraft mass, kg
ΔV = maneuver velocity change, km/s
χ = aeroshell mass fraction (aeroshell mass/total mass)

Introduction

AEROCAPTURE is an orbit insertion maneuver in which a spacecraft flies through a planetary atmosphere and uses drag force to decelerate and effect a hyperbolic to elliptical orbit change. Although this kind of guided hypersonic flight is more complicated to execute than conventional chemical propulsion orbit insertion, the prospect of large propellant mass savings has served to motivate development of aerocapture technology over the past four decades.[1–11] Sufficient technical maturity has been obtained to support a flight-test experiment in Earth orbit,[8] with a clear infusion path for subsequent robotic missions to Mars[6,7,9] and Titan[10] and manned missions to Mars.[5] It is expected that ongoing studies and research will produce similar technical maturity for aerocapture use at all other atmospheric worlds in the solar system.[11]

The net mass advantage of aerocapture equals the difference between propulsion system mass and aerocapture system mass for injecting the same payload into orbit. The essential character of this comparison is best illustrated with a first-order analysis in which the propulsion system mass is represented solely by the chemical propellant needed to effect the nominal orbit insertion velocity change ΔV, and the aerocapture system mass is represented solely by the mass of the aeroshell required to protect the spacecraft and provide the required aerodynamic characteristics. The result is shown in Fig. 1, where the before-to-after orbit insertion mass ratio of the spacecraft is plotted against the orbit insertion ΔV for the two approaches. The exponential curve for propulsion results directly from the rocket equation,

$$m_i/m_f = \exp(\Delta V/I_{sp}g_0) \tag{1}$$

The quasi-linear aerocapture curve in Fig. 1 is an estimate in which aeroshell mass fractions from past and present atmospheric entry missions are used as a proxy for aerocapture aeroshells at those planets. Table 1 summarizes the quantitative data used in this approach, where the aeroshell mass fraction is the ratio of the aeroshell mass to the total vehicle mass, and the nominal aerocapture ΔV corresponds to insertion into a low circular orbit at the planet. If χ represents the aeroshell mass fraction in Table 1, then the conversion to mass ratio in Fig. 1 follows from the simple algebraic equation

$$m_i/m_f = 1/(1-\chi) \tag{2}$$

Figure 1 clearly demonstrates the overwhelming mass advantage of aerocapture seen in the difference between the exponential curve and the quasi-linear curve. Even at the lowest ΔV of 2.4 km/s for Mars, aerocapture offers an advantage of $M_i/M_f = 2.2 - 1.3 = 0.9$, which represents almost a doubling of the orbiting spacecraft mass (and presumably a doubling of the science value) or almost a halving of the launch vehicle requirement. Either result is of enormous value in a field where significant technology improvements often provide a mass benefit of just a few kilograms.

Although the results in Fig. 1 are instructive, it is desirable to both increase the fidelity of the mass benefit analysis and to complement it by adding financial cost considerations. It is important to realize that aerocapture is just one of several steps required to place a spacecraft into orbit around a planet, and those other steps can have a significant impact on the mass and cost advantages afforded by aerocapture.

Presented as Paper 2003-4658 at the AIAA/ASME/SAE/ASEE 39th Joint Propulsion Conference, Huntsville, AL, 20–23 July 2003; received 25 July 2003; revision received 15 January 2004; accepted for publication 29 January 2004.

*Senior Engineer, Avionic Systems and Technology Division. Senior Member AIAA.
†Staff Engineer, Systems Division.
‡Senior Engineer, Systems Division. Member AIAA.

To cite one example, the use of a slower transfer ellipse to the outer solar system will reduce the orbit insertion ΔV, and hence the aeroshell mass, at the cost of a longer trip time. The challenge of evaluating the tradeoff between dissimilar attributes like smaller aeroshells vs longer trip times is one of the key motivators for adding monetary cost to the analysis. Although it is not the only metric for comparison, monetary cost does provide a quantitative measure that can be inclusive of the disparate elements required to place a spacecraft into a planetary orbit. One drawback to this approach is that monetary cost is an elusive variable. Historical and current costs are often viewed as proprietary information, and even when made available they are subject to questions about completeness and the existence of unusual circumstances that either inflated or decreased the actual cost. It is the premise of this study that, despite the inherent uncertainty in dealing with monetary costs, justifiable conclusions can be drawn about the benefits and cost effectiveness of aerocapture. As will be shown next, the quantitative results are not very sensitive to changes in the assumed cost and mass metrics for aerocapture, thus supporting the premise of being able to generate useful conclusions.

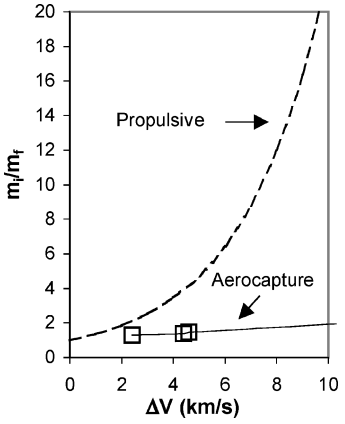

Fig. 1 Comparison of aerocapture to propulsive orbit insertion mass ratios.

Table 1 Historical database for aeroshell mass ratios

Entry mission	Planet/ moon	Entry date	Aeroshell mass fraction, %	Nominal aerocapture ΔV for a low circular orbit, km/s
Pioneer-Venus (L)	Venus	1978	31	4.6
Viking	Mars	1976	23	2.4
Pathfinder	Mars	1997	21	2.4
Galileo Probe	Jupiter	1995	60	17.0
Huygens	Titan	2005	27	4.4

The inclusion of monetary cost is one of four key differences between this study and prior efforts that quantified the benefits of aerocapture technology. The second difference is that the current study is focused on robotic missions to all possible aerocapture destinations in the solar system using a common methodology, thereby providing completeness and mission-to-mission consistency. In contrast, one prior study considered only manned missions to Mars,[5] another only manned missions to Mars and Venus,[1] whereas the third considered robotic missions only to Venus, Mars, and Saturn (although the aerodynamic deceleration was performed at Titan).[3] The third difference is that orbit insertion alternatives based on aerobraking, advanced chemical propulsion, and solar electric propulsion have been included in this study and quantitatively compared to aerocapture to more fairly represent the nonaerocapture options for future planetary missions. Finally, because the previous robotic aerocapture study occurred over two decades ago[3] updated values for aeroshell mass fractions, interplanetary trajectories, and launch-vehicle capabilities have been incorporated.

The net result of this study is a spacecraft mass delivered into orbit combined with a monetary cost for doing so in each mission scenario. With multiple aerocapture and nonaerocapture scenarios at all feasible destinations, it becomes possible to quantify the benefits of aerocapture across the solar system on both a mass and cost basis. The process also yields a dollar per kilogram delivery cost metric that facilitates planet-to-planet comparisons and future mission planning.

Aerocapture Mission Set

Aerocapture can, in principle, be used at any of the eight worlds in the solar system that have significant atmospheres. For each destination, there are an infinity of missions that can be performed corresponding to the infinity of possible orbits. Generally speaking, however, desirable spacecraft orbits for robotic missions tend to be of two kinds: low circular orbits suitable for planetary mapping and sample return missions and high eccentricity elliptical orbits suitable for combined planet and natural satellite observations. Mars Global Surveyor is an example of the former, while Galileo is an example of the latter. For the purpose of representing the spectrum of aerocapture missions in this study, we have defined a set of 11 missions across the eight destinations consisting of a circular orbit and/or an elliptical orbit at each world (Table 2). Note that some of these missions are taken directly from recent NASA strategic planning

Table 2 Aerocapture mission set

Label	Destination	Mission description	Nominal inertial entry speed, km/s	Nominal orbit insertion ΔV, km/s
V1	Venus	Low circular orbit (300 km) for mapping and sample return	11.7	4.6
V2	Venus	8,500 × 300-km elliptical orbit (e.g., Magellan)	11.7	3.3
E1	Earth	GTO to low-Earth-orbit aeroassisted transfer	10.3	2.3
M1	Mars	Low circular orbit (300 km) for mapping and sample return	5.9	2.4
M2	Mars	300 × 37,000-km elliptical orbit (e.g., Mars Odyssey preaerobraking)	5.9	1.2
J1	Jupiter	Low circular orbit (2000 km) inside the rings and radiation belt	59.0	17.0
J2	Jupiter	1,000 × 1,880,000-km elliptical orbit (apoapsis at Callisto)	59.0	1.4
S1	Saturn	120,000-km circular orbit for ring observations in the Cassini gap	35.0	8.0
T1	Titan	1,700-km circular orbit for mapping and aerobot/lander telecom relay	5.9	4.4
U1	Uranus	4,000 × 450,000-km elliptical orbit (apoapsis just beyond Titania)	24.0	4.5
N1	Neptune	4,000 × 430,000-km elliptical orbit (apoapsis just beyond Triton)	29.0	6.0

Table 3 Computation methodology for mass and cost

Element description	Mass calculation	Cost calculation
1) Launch from Earth at a specified C_3	Use NASA data for injected mass capability at specified C_3[a]; choose between small (Delta 2925), medium (Delta 4450, Atlas 5), and large (Delta 4050H) launchers	Use NASA provided data on estimated cost of the specified launch vehicle
2) Use of in-space propulsion	Rocket equation to compute propellant usage based on required ΔV; rules of thumb to estimate propulsion system dry mass and mass of supporting structure	Parametric cost curves based on propulsion system dry mass
3) Gravity assist maneuver(s)	Propellant mass for targeting maneuvers accounted for in step 2	No cost allocated, but trip time is accounted in step 4
4) In-space cruise	No mass allocated	Estimated cost per month for operations and ground support
5) Orbit insertion with propulsion	Rocket equation to compute propellant usage; rules of thumb to estimate propulsion system dry mass and mass of supporting structure	Parametric cost curves based on propulsion system dry mass
6) Aerobraking or aerocapture	No mass required for aerobraking; aerocapture mass fraction estimated from historical entry vehicle aeroshells (Fig. 1, Table 4)	Aerobraking: parametric cost curve for engineering and operations based on vehicle mass and ΔV Aerocapture: parametric cost curve based on vehicle mass
7) Postaerocapture periapse raise maneuver	Rocket equation to compute propellant usage; rules of thumb to estimate propulsion system dry mass and support structure	Parametric cost curves based on propulsion system dry mass

[a]Data available online at http://elvperf.ksc.nasa.gov/elvMap/staticPages/launch_vehicle_info.1.html.

documents,[12,13] whereas others represent less publicized missions or potentially unrecognized opportunities. It seems likely that some of these planetary missions will be NASA flagship missions, whereas others will be implemented through the smaller competitive programs like NASA Discovery, Mars Scout, and New Frontiers. The Earth mission listed is a special case of an aeroassisted orbit transfer from geosynchronous transfer orbit to low Earth orbit. Although not strictly an aerocapture maneuver, this mission involves the same flight characteristics and is expected to be the basis of an Earth orbit flight test experiment of aerocapture technology.[8] Potential applications include orbit transfer of secondary payloads launched to geosynchronous transfer orbit (GTO) and, in a small extrapolation, spacecraft returning from Lagrange points 4 and 5, the likely locations of future telescopes and space stations.

It has long been recognized that aerocapture can greatly reduce the launch mass required for the human exploration of Mars.[1,5] However, a manned mission to Mars is not included in this study primarily because the lack of existing very heavy lift launch vehicles precludes the mass and monetary cost analysis that was done for all of the robotic missions in the set.

Study Methodology

Mass and cost calculations for the missions in Table 2 were performed on spreadsheets using a host of input data, equations, and simplifying assumptions. Many cases were computed for each of the 11 missions consisting of a mixture of aerocapture and nonaerocapture scenarios so that direct comparisons could be made. The basic approach was to break down the mission architecture into a sequence of steps such that, given an injected mass capability of a particular launch vehicle, one could compute a delivered mass into the final working orbit at the destination. In this study, delivered mass is the useful spacecraft mass remaining after the aeroshell and other associated aerocapture elements have been discarded. This process is roughly akin to a staging calculation in that vehicle mass is consumed or discarded at each step of the way. The cost of the various elements was also computed based on simplified parametric models so that an overall total delivery cost could be determined. Table 3 lists the steps in the calculation for both mass and cost. Implicit in each mission calculation is a separate interplanetary trajectory analysis that provided the required C_3, trip time, and arrival velocity at the destination. Given that there are an infinity of possible trajectories for each mission, a single representative example was chosen after conducting a parametric study based on the common architectures.

Table 4 Propulsion values used in mass computations

Element	Value
Chemical propulsion module: dry mass/propellant mass	0.2
Solar-electric-propulsion module: dry mass/propellant mass	1.55
Stack support structural mass/propulsion module mass	0.05
State-of-the-art storable chemical propellant I_{sp}	325 s
Future advance storable chemical propellant I_{sp}^{a}	370 s
Solar-electric-propulsion specific impulse	4000 s

[a]Author's estimate. This value of 370 s is somewhat higher than currently identified systems but is intended to represent a best-case long-term performance goal.

Table 5 Aerocapture system mass fractions used in mass computations

Destination	Value
Venus	0.30
Earth	0.30
Mars	0.25
Jupiter	0.65
Saturn	0.55
Titan	0.35
Uranus	0.45
Neptune	0.45

The numerical data used in the mass calculations are given in Tables 4–6. Constant values with size are used for the chemical- and solar-electric-propulsion (SEP) system dry mass-to-propellant mass ratios with the understanding the ratios will be aggressive for very small systems and conservative for very large systems. The chemical-propulsion system specifications are derived from historical data. The SEP system specifications are derived from a mixture of historical and projected systems. Specifically, the DS-1 NSTAR engine[14–16] was used for the low-power Venus and Mars

scenarios, whereas all other trajectories used the next generation of ion thrusters, called NEXT.[17,18] The NSTAR engine is a 2.3-kW, 30-cm-diam engine with a maximum specific impulse I_{sp} of 3100 s and 130 kg of throughput per engine, whereas the NEXT engine is a 6.2-kW, 40-cm-diam engine with a maximum I_{sp} of 4000 s and 250 kg of throughput per engine. The solar array for the SEP system assumed a specific mass of 130 kg/kW for the 5–10-kW class trajectories and 150 kg/kW for the 25-kW class trajectories. The SEP system dry mass fraction also assumes 30% contingency on the dry mass and 10% contingency on the propellant mass. It is representative of a complete SEP module design and thus includes all of the structure, cabling, thermal, power, attitude control, feed system, tanks, thrusters, driving electronics, and redundancy that goes along with it.

To accommodate the very large number of cases in this study, it was necessary to use a simplified approach of specifying a single aerocapture system mass fraction for each planet as listed in Table 5. The values are estimates derived from the simple historical entry vehicle performance curve in Fig. 1 with approximately 0.05 added in each case to account for uncertainties and extra nonaeroshell components required for aerocapture. Examples of extra nonaeroshell components include telecommunications antennas that are discarded prior to atmospheric entry and heat-transfer equipment for thermal control of potential radioisotope power sources inside the aeroshell. Detailed designs and systems analyses have provided aerocapture mass fraction values for Earth[8] and Titan,[10] which are consistent with this simplified approach. However, those designs are based on blunt-body aeroshells of the type used in the historical entry database, and it must be stressed that at least the gas giant planet aerocapture missions will require more slender, higher lift-to-drag ratio shapes that can incur additional mass beyond what is estimated here. Conversely, the mass fraction values in Table 5 are conservative in the sense that they generally do not reflect the possible infusion of new aeroshell structural and thermal protection material technologies. Future detailed designs are required to determine which effects will prevail, designs that must factor in all of the details of mechanical layout, aerothermodynamics, flight mechanics, and the other pertinent disciplines that are ignored in this simplified methodology. Nevertheless, it will be shown that the advantages of aerocapture are not very sensitive to increases in the specific aerocapture mass fraction values used here, thereby indicating that upward revisions are not likely to invalidate the aerocapture mass advantage metrics computed in the following section.

Selected launch-vehicle injected (Earth departure) mass and C_3 data from the website http://elvperf.ksc.nasa.gov/elvMap/static Pages/launch_vehicle_info1.html are presented in Table 6.

The cost input data summarized in Table 7 are comprised of a mixture of well-defined publicized costs, published and unpublished studies, anecdotal evidence, and educated guesses. No attempt has been made to include the effects of monetary inflation in this analysis, and so the costs in Table 7 are essentially current year (2004) costs. Fixed values are used for the launch vehicles, a per-month cost for operations and ground support during in-space cruise, and square-root parametric costs as a function of mass for the other elements, that is, in-space propulsion, propulsion module-to-aeroshell interface structure, aerobraking, and aerocapture. Aerobraking costs are also linearly scaled with the ΔV required for orbit circularization. The use of a square-root function to represent the cost vs mass relationship is a simplification that is intended to capture the essential feature that larger systems cost more but that economies of scale limit that growth to a less-than-linear dependence. Where possible, these square-root cost curves have been anchored to at least one

Table 6 Launch-vehicle injected mass vs C_3[a]

	Injected mass, kg	
Launch-vehicle	$C_3 = 10$ km^2/s^2	$C_3 = 30$ km^2/s^2
Delta 2925H	1200	N/A
Delta 4450	3690	2200
Atlas 531	4340	2970
Delta 4050-H	7810	5220

[a]Data available online at http://elvperf.ksc.nasa.gov/elvMap/static Pages/launch_vehicle_info.1.html.

Table 7 Numerical values used in cost computations

	Cost $= a + bx^{0.5}$				
Element	a	b	x	Unit	Source/justification
Delta 2925H	88	N/A	N/A	\$M	Data available online[a]
Delta 4450/Atlas V	140	N/A	N/A	\$M	Data available online[a]
Delta 4050H	232	N/A	N/A	\$M	Data available online[a]
Cruise operations cost	18	N/A	N/A	\$M/year	Author's estimate (includes low-level science team support)
SOA chemical propulsion	2	1.7	Dry mass of prop. system, kg	\$M	Unpublished estimate[b]
Advanced chemical propulsion	3	2.55	Dry mass of prop. system, kg	\$M	Author's estimate that advanced chemical will be 50% more costly than SOA chemical
Solar electric propulsion	40	0.8	Dry mass of prop. system, kg	\$M	Private communication[c]
Aeroshell: prop. module interface structure	2	0.5	Interface structure mass, kg	\$M	Author's estimate
Aerobraking mass function	5	0.2	Mass of delivered spacecraft, kg	\$M	Private communication[d]
Aerobraking ΔV coefficient	$\Delta V/1.2$	N/A	Mass of delivered spacecraft, kg	N/A	Assumes cost linearly scales with ΔV
Aerocapture	7	0.8	Aeroshell mass, kg	\$M	Unpublished data[e]

[a]http://newfrontiers.larc.nasa.gov/newfrontiers/Ao-New_Frontiers-ELV_Summ_3a.pdf. The cost data in this document are the best currently available for launch vehicles used in planetary exploration missions.
[b]Jet Propulsion Laboratory, Feb. 2003. Unpublished estimate that a Cassini bipropellant system rebuild (500-kg dry mass) would cost \$40m. The cost model gives $2 + 1.7 \times 500^{0.5} =$ \$40m.
[c]J. R. Brophy, private communication, Feb. 2003. He estimated that a 25-kw, 800-kg dry mass SEP system based on advanced NSTAR technology from DS-1 would cost \$63M. The cost model gives $40 + 0.8 \times 800^{0.5} =$ \$63M.
[d]R. A. Mase, private communication. Mars Odyssey data indicate that aerobraking for the 600-kg spacecraft had a cost of \$9.3M including planning, development, operations and science team during the three-month aerobraking period. The cost model gives $5 + 0.2 \times 600^{0.5} =$ \$9.9M.
[e]J. L. Hall, unpublished data from the design described in Ref. 7. The estimated cost of the AFTE aerocapture system was \$12.8M including the design, analysis, simulation, aeroshell fabrication, system integration, and testing. Because the AFTE aeroshell was approximately 50 kg, the model gives $7 + 0.8 \times 50^{0.5} =$ \$12.7M.

data point from either a historical mission or recent detailed studies (see footnotes to Table 7). These square-root cost functions are plotted in Fig. 2.

The cost estimates in this study do not include technology development costs for elements not yet ready for flight, namely, aerocapture, advanced chemical, and advanced SEP. Furthermore, in the case of aerocapture, no attempt is made to distinguish the cost differences between different aeroshell shapes or different thermal protection materials of the same overall aeroshell mass. The impact of these simplifications will be discussed in the next section.

Results and Discussion

This study generated a very large amount of data, the essential elements of which are presented in this paper. Figures 3a–3j show plots of delivered mass versus delivery cost for all 10 non-Earth missions listed in Table 2. The 11th mission, aeroassisted orbit transfer at Earth, will be treated separately at the end of the section. Each figure is a scatter plot comprised of multiple scenarios where the symbols are used to denote the method of orbit insertion: 1) filled diamonds for state-of-the-art chemical propulsion with an $I_{sp} = 325$ s, 2) open diamonds for advanced chemical propulsion with an $I_{sp} = 370$ s, 3) stars for aerobraking, 4) filled circles for aerocapture, and 5) filled squares for solar electric propulsion. Note that negative mass values in the plots denote non-feasible scenarios.

Tables 8–10 provide the raw data for each computed scenario, listing the trip time, delivered mass and delivered cost, respectively.

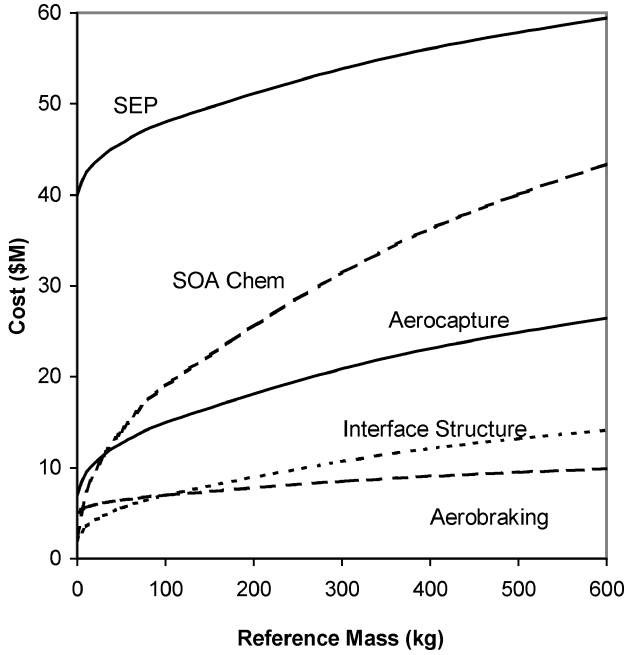

Fig. 2 Square-root cost functions.

Table 8 Trip times for all mission scenarios

No.	Launch vehicle	Transit propulsion	Gravity assist	Orbit insertion	Mission and trip time, years									
					V1	V2	M1	M2	J1	J2	S1	T1	U1	N1
1	Delta 2925	None	None	chem325	0.5	0.5	0.8	0.8	—	—	—	—	—	—
2	Delta 2925	None	None	chem370	0.5	0.5	0.8	0.8	—	—	—	—	—	—
3	Delta 2925	None	None	A/B	0.5	0.5	0.8	0.8	—	—	—	—	—	—
4	Delta 2925	None	None	A/C	0.5	0.5	0.8	0.8	—	—	—	—	—	—
5	Delta 4450	None	None	chem325	0.5	0.5	0.8	0.8						
6	Delta 4450	None	None	chem370	0.5	0.5	0.8	0.8	—	—	—	—	—	—
7	Delta 4450	None	None	A/B	0.5	0.5	0.8	0.8	—	—	—	—	—	—
8	Delta 4450	None	None	A/C	0.5	0.5	0.8	0.8	—	—	—	—	—	—
9	Delta 4450	chem325	V/E	chem325	—	—	—	—	6.1	6.1	7.5	7.5	—	—
10	Delta 4450	chem370	V/E	chem370	—	—	—	—	6.1	6.1	7.5	7.5	—	—
11	Delta 4450	chem325	V/E	A/C	—	—	—	—	6.1	6.1	7.5	7.5	—	—
12	Delta 4450	chem325	V/E + J	chem325	—	—	—	—	—	—	—	—	9.0	10.7
13	Delta 4450	chem325	V/E + J	chem370	—	—	—	—	—	—	—	—	9.0	10.7
14	Delta 4450	chem325	V/E + J	A/C	—	—	—	—	—	—	—	—	9.0	10.7
15	Delta 4450	SEP	V/E	chem325	—	—	—	—	3.5	3.5	6.0	6.0	8.0	10.5
16	Delta 4450	SEP	V/E	chem370	—	—	—	—	3.5	3.5	6.0	6.0	8.0	10.5
17	Delta 4450	SEP	V/E	A/C	—	—	—	—	3.5	3.5	6.0	6.0	8.0	10.5
18	Delta 4450	SEP	V/E + J	chem325	—	—	—	—	—	—	6.7	6.7	8.4	—
19	Delta 4450	SEP	V/E + J	chem370	—	—	—	—	—	—	6.7	6.7	8.4	—
20	Delta 4450	SEP	V/E + J	A/C	—	—	—	—	—	—	6.7	6.7	8.4	—
21	Atlas 551	SEP	V/E + J	chem325	—	—	—	—	—	—	—	—	—	10.5
22	Atlas 551	SEP	V/E + J	chem370	—	—	—	—	—	—	—	—	—	10.5
23	Atlas 551	SEP	V/E + J	A/C	—	—	—	—	—	—	—	—	—	10.5
24	Delta 4050H	None	None	chem325	0.5	0.5	0.8	0.8	2.2	2.2	—	—	9.0	—
25	Delta 4050H	None	None	chem370	0.5	0.5	0.8	0.8	2.2	2.2	—	—	9.0	—
26	Delta 4050H	None	None	A/B	0.5	0.5	0.8	0.8	—	—	—	—	—	—
27	Delta 4050H	None	None	A/C	0.5	0.5	0.8	0.8	2.2	2.2	—	—	9.0	—
28	Delta 4050H	chem325	V/E	chem325	—	—	—	—	6.1	6.1	7.5	7.1	—	—
29	Delta 4050H	chem370	V/E	chem370	—	—	—	—	6.1	6.1	7.5	7.1	—	—
30	Delta 4050H	chem325	V/E	A/C	—	—	—	—	6.1	6.1	7.5	7.1	—	—
31	Delta 4050H	chem325	V/E + J	chem325	—	—	—	—	—	—	7.7	6.7	9.0	10.7
32	Delta 4050H	chem370	V/E + J	chem370	—	—	—	—	—	—	7.7	6.7	9.0	10.7
33	Delta 4050H	chem325	V/E + J	A/C	—	—	—	—	—	—	7.7	6.7	9.0	10.7
34	Delta 4050H	SEP	V/E	chem325	—	—	—	—	4.0	4.0	6.0	6.0	8.0	10.5
35	Delta 4050H	SEP	V/E	chem370	—	—	—	—	4.0	4.0	6.0	6.0	8.0	10.5
36	Delta 4050H	SEP	V/E	A/C	—	—	—	—	4.0	4.0	6.0	6.0	8.0	10.5
37	Delta 4050H	SEP	V/E + J	chem325	—	—	—	—	—	—	6.7	6.7	8.4	10.5
38	Delta 4050H	SEP	V/E + J	chem370	—	—	—	—	—	—	6.7	6.7	8.4	10.5
39	Delta 4050H	SEP	V/E + J	A/C	—	—	—	—	—	—	6.7	6.7	8.4	10.5
40	Delta 4050H	SEP	None	SEP	2.5	2.2	1.4	1.4	—	—	—	—	—	—
41	Delta 4450	SEP	None	SEP	2.4	2.1	1.5	1.3	—	—	—	—	—	—
42	Delta 2925	SEP	None	SEP	2.5	2.2	1.3	1.2	—	—	—	—	—	—

Table 9 Delivered mass for all mission scenarios

No.	Launch vehicle	Transit propulsion	Gravity assist	Orbit insertion	Mission and deliver mass, kg									
					V1	V2	M1	M2	J1	J2	S1	T1	U1	N1
1	Delta 2925	None	None	chem325	105	275	432	729	——	——	——	——	——	——
2	Delta 2925	None	None	chem370	171	344	495	774	——	——	——	——	——	——
3	Delta 2925	None	None	A/B	265	275	702	729	——	——	——	——	——	——
4	Delta 2925	None	None	A/C	788	788	807	807	——	——	——	——	——	——
5	Delta 4450	None	None	chem325	318	835	1309	2210	——	——	——	——	——	——
6	Delta 4450	None	None	chem370	519	1046	1499	2344	——	——	——	——	——	——
7	Delta 4450	None	None	A/B	804	835	2128	2210	——	——	——	——	——	——
8	Delta 4450	None	None	A/C	2395	2395	2444	2444	——	——	——	——	——	——
9	Delta 4450	chem325	V/E	chem325	——	——	——	——	−652	2007	−130	208	——	——
10	Delta 4450	chem370	V/E	chem370	——	——	——	——	−634	2143	−93	304	——	——
11	Delta 4450	chem325	V/E	A/C	——	——	——	——	1048	1048	129	762	——	——
12	Delta 4450	chem325	V/E + J	chem325	——	——	——	——	——	——	——	——	166	−98
13	Delta 4450	chem325	V/E + J	chem370	——	——	——	——	——	——	——	——	287	−45
14	Delta 4450	chem325	V/E + J	A/C	——	——	——	——	——	——	——	——	912	681
15	Delta 4450	SEP	V/E	chem325	——	——	——	——	−385	1089	−200	231	294	42
16	Delta 4450	SEP	V/E	chem370	——	——	——	——	−374	1176	−143	330	378	93
17	Delta 4450	SEP	V/E	A/C	——	——	——	——	619	619	179	1059	748	481
18	Delta 4450	SEP	V/E + J	chem325	——	——	——	——	——	——	−260	127	239	——
19	Delta 4450	SEP	V/E + J	chem370	——	——	——	——	——	——	−192	242	349	——
20	Delta 4450	SEP	V/E + J	A/C	——	——	——	——	——	——	222	1315	1005	——
21	Atlas 551	SEP	V/E + J	chem325	——	——	——	——	——	——	——	——	——	−52
22	Atlas 551	SEP	V/E + J	chem370	——	——	——	——	——	——	——	——	——	32
23	Atlas 551	SEP	V/E + J	A/C	——	——	——	——	——	——	——	——	——	901
24	Delta 4050H	None	None	chem325	675	1770	2802	4693	−454	1339	——	——	103	——
25	Delta 4050H	None	None	chem370	1101	2218	3208	4983	−441	1438	——	——	340	——
26	Delta 4050H	None	None	A/B	1705	1770	4556	4693	——	——	——	——	——	——
27	Delta 4050H	None	None	A/C	5078	5078	5232	5232	729	729	——	——	113	——
28	Delta 4050H	chem325	V/E	chem325	——	——	——	——	−1407	4334	−294	472	——	——
29	Delta 4050H	chem370	V/E	chem370	——	——	——	——	−1369	4628	−211	691	——	——
30	Delta 4050H	chem325	V/E	A/C	——	——	——	——	2262	2262	292	1731	——	——
31	Delta 4050H	chem325	V/E + J	chem325	——	——	——	——	——	——	−485	253	357	−222
32	Delta 4050H	chem370	V/E + J	chem370	——	——	——	——	——	——	−353	502	618	−102
33	Delta 4050H	chem325	V/E + J	A/C	——	——	——	——	——	——	494	2630	1966	1543
34	Delta 4050H	SEP	V/E	chem325	——	——	——	——	−579	1709	−311	278	115	113
35	Delta 4050H	SEP	V/E	chem370	——	——	——	——	−563	1835	−222	429	237	180
36	Delta 4050H	SEP	V/E	A/C	——	——	——	——	930	930	278	1645	1175	601
37	Delta 4050H	SEP	V/E + J	chem325	——	——	——	——	——	——	−439	244	179	−78
38	Delta 4050H	SEP	V/E + J	chem370	——	——	——	——	——	——	−323	441	366	81
39	Delta 4050H	SEP	V/E + J	A/C	——	——	——	——	——	——	375	2218	1819	1680
40	Delta 4050H	SEP	None	SEP	2834	3542	3471	4222	——	——	——	——	——	——
41	Delta 4450	SEP	None	SEP	1412	1760	2168	2607	——	——	——	——	——	——
42	Delta 2925	SEP	None	SEP	221	366	508	660	——	——	——	——	——	——

In these tables, V/E denotes one or more Venus and/or Earth gravity assists, J denotes a Jupiter gravity assist, chem325 and chem370 denote chemical propulsion with a 325- or 370-s specific impulse, respectively, A/B denotes aerobraking, A/C denotes aerocapture, and SEP denotes solar electric propulsion. Note that aerobraking results are not provided for outer planet missions because they do not offer an advantage: either the target orbit is highly elliptical (J2, U1, N1), or most of the orbit insertion ΔV corresponds to the orbit capture itself and not the orbit circularization.

There are several noteworthy results illustrated in Fig. 3. Perhaps the most important is that the aerocapture data points (filled circles) generally lie to the right of the nonaerocapture points, thus confirming the expectation (Fig. 1) that aerocapture possesses a mass advantage over other orbit insertion techniques. This advantage is small when the orbit insertion velocity change is small (e.g., Mission M1, $\Delta V = 2.4$ km/s), and it is large when the orbit insertion velocity change is large (e.g., Mission N1, $\Delta V = 5$–7 km/s). Note that the Jupiter low-circular-orbit mission (J1) and the Saturn ring-observer mission (S1) are so challenging that they do not show any nonaerocapture scenarios with a positive delivered mass. For these missions aerocapture is truly enabling, a description that can also be applied to the Neptune orbiter mission (N1) because the maximum nonaerocapture delivered mass of 180 kg (scenario 35) is too small for a practical deep space orbiter. In contrast, the Mars high-eccentricity mission (M2) shows essentially no benefit with aerocapture, and the Jupiter high-eccentricity orbit mission (J2) shows that aerocapture actually delivers less mass than some nonaerocapture architectures. The explanation for Jupiter is that the high-entry velocities require large aeroshell mass fractions (∼65%) to protect the spacecraft, but this mass cannot be recouped in propellant savings because the orbit insertion ΔV is only ∼1.4 km/s. The same logic applies to mission M2 although in this case the propellant savings are equal to the aerocapture system mass so that no advantage or disadvantage results. For all other missions aerocapture improves, and often substantially improves, the ability to deliver mass into the desired orbit. Results for all missions are presented in Table 11, where the best aerocapture and nonaerocapture options are directly compared for the same heavy lift-launch vehicle. To highlight just one example, the Titan orbiter scenario 33 provides a factor of 3.8 improvement in delivered mass vs the best alternative, scenario 29 (2630 vs 691 kg). Note that if the delivered mass requirements for Titan and Uranus are sufficiently large (approximately greater than 600–700 kg), then aerocapture becomes an enabling, and not just enhancing, technology for them based on the mass limit of the Delta IV heavy launch vehicle. Another notable result is that the use of solar electric propulsion to achieve orbit at Venus and Mars shows worse performance than aerocapture, despite the relatively high solar flux and extraordinary specific impulse of SEP. This is because of a combination of the high dry mass inherent to SEP designs and the significant gravity losses associated with long-duration spiral trajectories into orbit.

The mass advantage of aerocapture vs chemical propulsion ($I_{sp} = 325$ s) orbit insertion computed in this study generally agrees with the prior work for robotic missions reported in Ref. 3. For Mars,

Table 10 Total delivery cost for all mission scenarios

No.	Launch vehicle	Transit propulsion	Gravity assist	Orbit insertion	Mission and delivery cost SM									
					V1	V2	M1	M2	J1	J2	S1	T1	U1	N1
1	Delta 2925	None	None	chem325	122	120	123	119	——	——	——	——	——	——
2	Delta 2925	None	None	chem370	133	129	133	126	——	——	——	——	——	——
3	Delta 2925	None	None	A/B	128	120	129	119	——	——	——	——	——	——
4	Delta 2925	None	None	A/C	126	126	131	135	——	——	——	——	——	——
5	Delta 4450	None	None	chem325	191	188	189	182	——	——	——	——	——	——
6	Delta 4450	None	None	chem370	210	205	205	193	——	——	——	——	——	——
7	Delta 4450	None	None	A/B	198	188	196	182	——	——	——	——	——	——
8	Delta 4450	None	None	A/C	194	194	197	203	——	——	——	——	——	——
9	Delta 4450	chem325	V/E	chem325	——	——	——	——	298	279	317	315	——	——
10	Delta 4450	chem370	V/E	chem370	——	——	——	——	321	291	335	331	——	——
11	Delta 4450	chem325	V/E	A/C	——	——	——	——	306	306	338	330	——	——
12	Delta 4450	chem325	V/E + J	chem325	——	——	——	——	——	——	——	——	349	374
13	Delta 4450	chem325	V/E + J	chem370	——	——	——	——	——	——	——	——	369	392
14	Delta 4450	chem325	V/E + J	A/C	——	——	——	——	——	——	——	——	368	390
15	Delta 4450	SEP	V/E	chem325	——	——	——	——	314	301	353	350	383	428
16	Delta 4450	SEP	V/E	chem370	——	——	——	——	332	311	369	363	394	439
17	Delta 4450	SEP	V/E	A/C	——	——	——	——	322	322	372	356	392	436
18	Delta 4450	SEP	V/E + J	chem325	——	——	——	——	——	——	368	366	393	——
19	Delta 4450	SEP	V/E + J	chem370	——	——	——	——	——	——	386	381	407	——
20	Delta 4450	SEP	V/E + J	A/C	——	——	——	——	——	——	388	370	401	——
21	Atlas 551	SEP	V/E + J	chem325	——	——	——	——	——	——	——	——	——	431
22	Atlas 551	SEP	V/E + J	chem370	——	——	——	——	——	——	——	——	——	446
23	Atlas 551	SEP	V/E + J	A/C	——	——	——	——	——	——	——	——	——	438
24	Delta 4050H	None	None	chem325	301	297	296	286	312	298	——	——	467	——
25	Delta 4050H	None	None	chem370	329	322	318	302	331	308	——	——	496	——
26	Delta 4050H	None	None	A/B	310	297	303	286	——	——	——	——	——	——
27	Delta 4050H	None	None	A/C	302	302	305	305	320	320	——	——	482	——
28	Delta 4050H	chem325	V/E	chem325	——	——	——	——	410	383	429	418	——	——
29	Delta 4050H	chem370	V/E	chem370	——	——	——	——	443	400	455	441	——	——
30	Delta 4050H	chem325	V/E	A/C	——	——	——	——	419	419	456	437	——	——
31	Delta 4050H	chem325	V/E + J	chem325	——	——	——	——	——	——	433	412	462	486
32	Delta 4050H	chem370	V/E + J	chem370	——	——	——	——	——	——	460	436	489	511
33	Delta 4050H	chem325	V/E + J	A/C	——	——	——	——	——	——	461	426	486	505
34	Delta 4050H	SEP	V/E	chem325	——	——	——	——	425	408	457	453	489	532
35	Delta 4050H	SEP	V/E	chem370	——	——	——	——	446	420	476	469	505	543
36	Delta 4050H	SEP	V/E	A/C	——	——	——	——	433	433	478	458	496	540
37	Delta 4050H	SEP	V/E + J	chem325	——	——	——	——	——	——	476	472	503	542
38	Delta 4050H	SEP	V/E + J	chem370	——	——	——	——	——	——	498	491	522	562
39	Delta 4050H	SEP	V/E + J	A/C	——	——	——	——	——	——	499	476	510	549
40	Delta 4050H	SEP	None	SEP	367	360	334	330	——	——	——	——	——	——
41	Delta 4450	SEP	None	SEP	258	252	235	228	——	——	——	——	——	——
42	Delta 2925	SEP	None	SEP	196	190	169	166	——	——	——	——	——	——

Table 11 Delivered mass summary for heavy launch vehicle

Mission	Best A/C mass, kg	Best non-A/C mass, kg	% Increase	What is best non-A/C?
Venus V1	5078	2834	79	all-SEP
Venus V2	5078	3542	43	all-SEP
Mars M1	5232	4556	15	A/B
Mars M2	5232	4983	5	chem370
Jupiter J1	2262	< 0	Infinite	N/A
Jupiter J2	2262	4628	−51	chem370
Saturn S1	494	< 0	Infinite	N/A
Titan T1	2630	691	280	chem370
Uranus U1	1966	618	218	chem370
Neptune N1	1680	180	832	chem370

the current study shows a factor of 1.87 (mission M1, scenario 8 vs scenario 5) compared to the Ref. 3 values, which range from 1.8 to 1.9. For Venus, the current study shows a factor of 2.86 (mission V2, scenario 8 vs scenario 5) compared to the Ref. 3 values, which range from 2.4 to 5.8. Although Ref. 3 also analyzed a Saturn/Titan mission, it consisted of high-speed aerodynamic deceleration at Titan for the purpose of achieving orbit at Saturn, an architecture not considered in the current study and therefore not one for which direct comparisons can be made. Direct comparisons to the manned Mars results of Ref. 5 and the manned Mars and Venus results in Ref. 1 also cannot be made because of the differences in mission architecture (the return to Earth element), vehicle size (up to 200 t), and propulsion baselines (nuclear thermal and $I_{sp} = 480$ s storable cryogenic chemical propulsion).

Unlike the mass data for many missions, the cost data do not show dramatic many-fold improvements as a result of the use of aerocapture. The reason is that the orbit insertion costs are just a small fraction (10–20%) of the overall delivery costs because of the dominating effect of launch vehicle, multiyear operations, and, where applicable, in-space chemical- or solar-electric-propulsion module costs. Moreover, the projected cost of aerocapture systems are comparable to the cost of chemical-propulsion systems for orbit insertion, so that any aerocapture advantage generally results from shorter trip times or smaller launch vehicles, advantages that cannot produce large cost reductions on a percentage basis. Nevertheless, in absolute terms the savings of tens of millions of dollars or more can be critical to the success of competed missions in a cost-constrained environment. For example, a ∼700-kg Titan orbiter can be delivered for $441M without aerocapture (scenario 29) or $330M with aerocapture (scenario 11), where the higher cost is due to a larger launch vehicle and substantial in-space propulsion. The savings of $111M is significant in absolute terms, but on a percentage basis is only 25% of the total delivery cost for the mission. Another notable result seen in the data is that each mission has a minimum delivery cost corresponding to the smallest available launch vehicle, one that is mostly independent of the orbit insertion technique. These minimum costs range from approximately $120M for Venus and Mars, to $320M for Saturn and Titan, to $390M for Neptune.

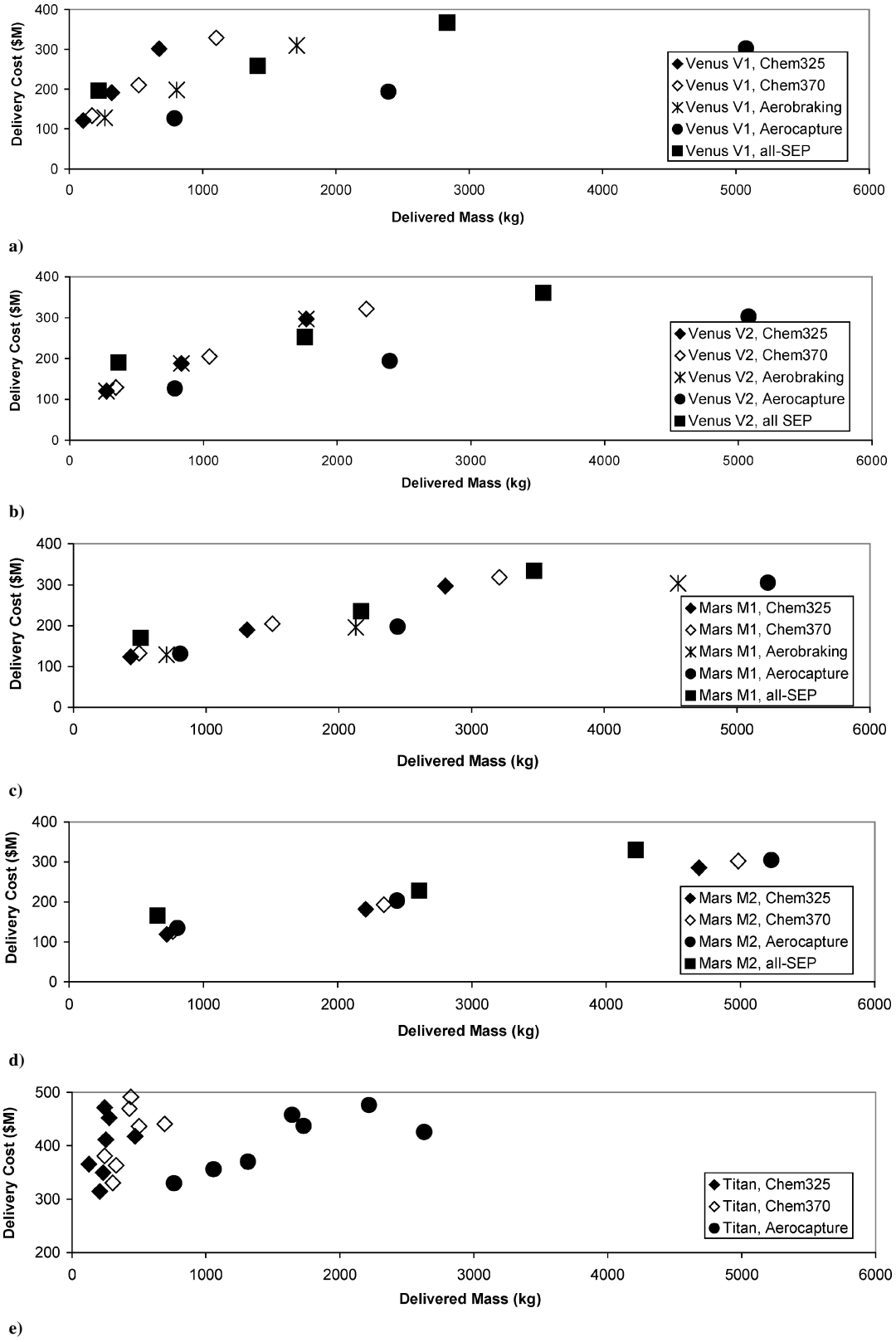

Fig. 3 Delivered mass vs delivery cost for all non-Earth missions.

Table 12 presents a dollar/kilogram metric for each mission using the best aerocapture and best nonaerocapture scenarios in both the medium- and heavy-launch vehicle categories. The data for the medium launch vehicle are also plotted in Fig. 4. It can be seen in Table 12 that although the economy of scale produces lower dollar/kilogram costs for the heavy-launch vehicle, the percentage reduction offered by aerocapture technology is largely independent of the launch vehicle size. This percentage reduction in delivery cost is substantial for the seven missions (V1, V2, J1, S1, T1, U1, and N1) with a large orbit insertion ΔV requirement, ranging from a 41 to 100% on a dollar per unit mass basis. In this context, a 100% reduction corresponds to a mission that cannot be done without aerocapture. The high-eccentricity Mars (M2) and Jupiter (J2) missions are not helped by aerocapture, as just discussed, while the low-circular-orbit M1 mission shows a modest delivery cost reduction of 12 or 13% for the medium- and heavy-launch vehicles, respectively.

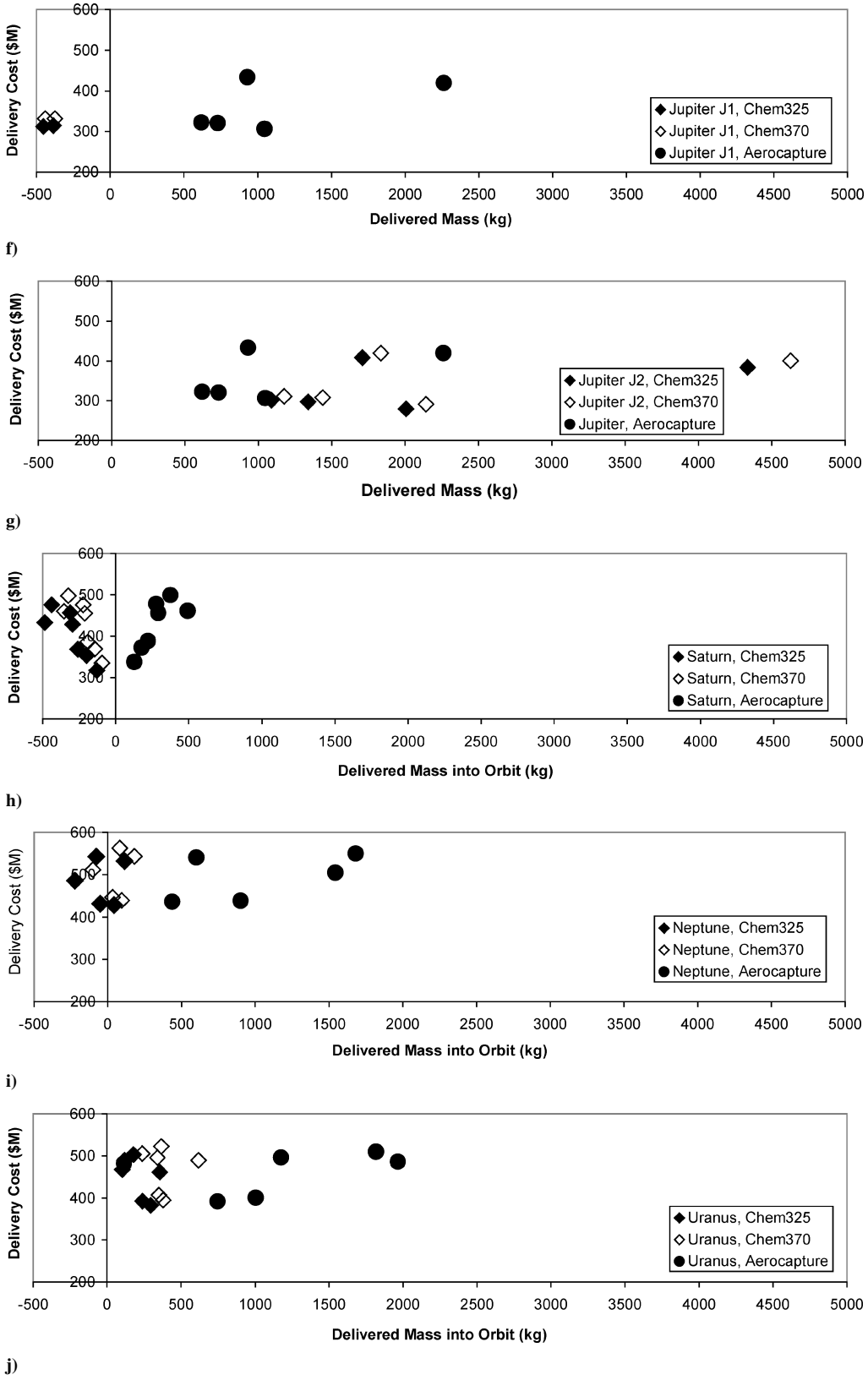

Fig. 3 Delivered mass vs delivery cost for all non-Earth missions (continued).

One way to put the magnitude of the aerocapture performance improvements into perspective is to compute the equivalent propulsion system specific impulse that would be required to match the aerocapture delivered mass with a non-aerocapture approach. The results are shown in Table 13, where, except for M2 and J2 missions that are not helped by aerocapture, the required specific impulse exceeds any available or planned storable chemical propulsion system. Note that the relatively low required specific impulse for the Saturn ring-observer mission reflects the fact that it requires a large 3.3-km/s periapse raise maneuver to circularize the orbit in the Cassini gap of the rings, and therefore direct propulsive orbit insertion with a much improved specific impulse will also save all of the propellant associated with this large maneuver.

The performance advantages of aerocapture for most of the missions in this set are so large that they are not significantly compromised by signficant increases in the predicted aerocapture system

Table 12 Summary of $M/kg metrics for all missions

Mission	Medium-launch vehicle				Heavy-launch vehicle			
	Best A/C	Best non-A/C	% Reduction	What is best non-A/C?	Best A/C	Best non-A/C	% Reduction	What is best non-A/C?
Venus V1	0.08	0.18	56	all-SEP	0.06	0.13	54	all-SEP
Venus V2	0.08	0.14	44	all-SEP	0.06	0.10	41	all-SEP
Mars M1	0.08	0.09	12	A/B	0.06	0.07	13	A/B
Mars M2	0.08	0.08	−1	chem325	0.06	0.06	4	chem325
Jupiter J1	0.29	N/A	100	N/A	0.19	N/A	100	N/A
Jupiter J2	0.29	0.14	−115	chem370	0.19	0.09	−115	chem370
Saturn S1	1.75	N/A	100	N/A	0.93	N/A	100	N/A
Titan T1	0.28	1.09	74	chem370	0.16	0.64	75	chem370
Uranus U1	0.40	1.04	62	chem370	0.25	0.79	69	chem370
Neptune N1	0.49	4.74	90	chem370	0.33	3.01	89	chem370

Table 13 Required specific impulse to match aerocapture performance

Mission	Equivalent I_{sp}, s
Venus V1	1060
Venus V2	970
Mars M1	455
Mars M2	——
Jupiter J1	2040
Jupiter J2	——
Saturn S1	640
Titan T1	1240
Uranus U1	815
Neptune N1	1140

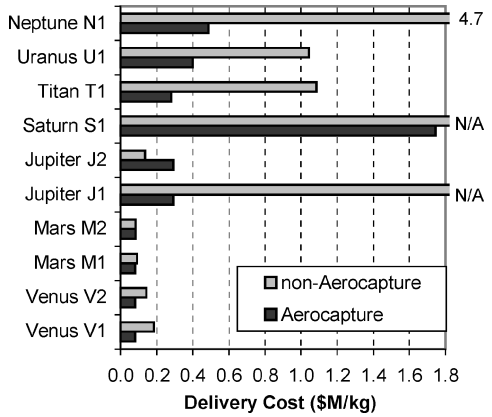

Fig. 4 Best scenario delivery costs per unit mass for a medium-launch vehicle.

mass fraction or cost. Table 14 shows the results of a sensitivity study based on medium-launch vehicles in which either the aerocapture system mass or the aerocapture system cost was increased by 30% while holding all other parameters constant. The change in percentage cost reduction using aerocapture on a dollar/kilogram delivery basis is small in all cases except for the M1 mission where a mass increase of this size eliminates the modest aerocapture advantage. Note also that the increased mass effect always causes a greater change than increased cost, which is just a reflection of the fact that aerocapture costs are only a small fraction of the overall delivery cost. The conclusion is that most of the projected aerocapture advantage on a dollar/kilogram delivery basis will be retained even in the event that the mass or cost of aerocapture technology is 30% greater than estimated in this study. This sensitivity result helps to justify the use of highly simplified mass and cost models for aerocapture as described in the preceding section in that errors of up to +30% (and more) will not alter the conclusion that aerocapture provides a substantial advantage for many missions. Conversely, improvements resulting from superior-than-expected aerocapture mass or cost performance will also be small on a percentage basis; however, on a net basis the potential savings of many millions of dollars

Table 14 Sensitivity of the aerocapture advantage (medium-launch vehicle scenarios)

Mission	Aerocapture delivery cost reduction		
	Nominal case, %	+30% A/C mass, %	+30% A/C cost, %
Venus V1	56	49	53
Venus V2	44	36	41
Mars M1	12	1	8
Mars M2	——	——	——
Jupiter J1	100	100	100
Jupiter J2	——	——	——
Saturn S1	100	100	100
Titan T1	74	69	74
Uranus U1	62	49	61
Neptune N1	90	86	90

Table 15 Projected spacecraft mass increases for aerocapture-enhanced missions

Mission	Non-A/C $M/kg for heavy launcher	A/C $M/kg for heavy launcher	Delivery cost, $M	Mass increase per spacecraft, kg
V1	0.13	0.06	300	2722
V2	0.10	0.06	300	2086
M1	0.07	0.06	300	648
T1	0.64	0.16	440	2028
U1	0.69	0.25	500	1298

should still serve as a powerful motivator for producing efficient aerocapture systems.

Based on the planetary results just presented, it is possible to categorize the aerocapture missions into three groups: enabled (J1, S1, N1), enhanced (V1, V2, M1, T1, U1), and not helped (M2, J2). For the enhanced category, the aerocapture benefit can manifest itself in a reduced delivery cost, an increased spacecraft mass, or a combination of the two. The preferred optimization will necessarily depend on the details of any given mission, but results for the two limits are presented in Tables 15 and 16. For the fixed cost limit in Table 15, the heavy-launch vehicle mass and cost data are used for each of the five missions to produce a net delivered mass increase. This mass increase is equivalent to the horizontal distance between the aerocapture and nonaerocapture data points on the appropriate mission plots in Fig. 3. Similarly, the fixed mass limit can be obtained by measuring the vertical distance between the aerocapture and nonaerocapture data points in Fig. 3, which for the Venus and Mars missions happens to correspond to the difference between the million-dollar/kilogram cost of aerocapture with a medium-launch vehicle and the best nonaerocapture cost on a heavy launch vehicle (Table 16). However, this method breaks down with the Titan and Uranus missions because there are not any nonaerocapture scenarios that can deliver as much mass as the most efficient aerocapture scenarios based on a medium-launch vehicle. Therefore, we have estimated a million-dollar/kilogram cost of a hypothetical

Table 16 Projected cost savings for aerocapture-enhanced missions

Mission	Non-A/C $M/kg for heavy launcher	A/C $M/kg for medium launcher	Spacecraft mass, kg	Cost savings per spacecraft, $M
V1	0.13	0.08	2400	116
V2	0.10	0.08	2400	50
M1	0.07	0.08	2400	−34
T1[a]	0.36	0.28	1300	102
U1[a]	0.49	0.40	1000	91

[a]Estimated $M/kg value for an hypothetical ultraheavy-launch vehicle that can deliver the listed spacecraft mass.

ultraheavy-launch vehicle that could deliver sufficient mass in the T1 and U1 nonaerocapture scenarios. Note that these delivery costs must reflect economies of scale and therefore are significantly better than those based on existing heavy vehicles; however, they do not include the sizable research and development costs associated with any new launch vehicle. With these caveats, it can be seen that four of the five missions show a cost savings, with values ranging from $50M for the Venus V2 mission to $116M for the Venus V1 mission. The Mars M1 mission does not show a cost savings because the size scaling dilution effect is larger than the aerocapture performance benefit. This suggests that the primary use of aerocapture at Mars will be to increase the spacecraft mass for a fixed delivery system as shown in Table 15.

One caveat to this conclusion is that Mars missions are amenable to comanifesting, that is, sending two spacecraft using a single large launch vehicle rather than two smaller launch vehicles. For example, aerocapture would allow a single Delta IV heavy to send a pair of 2500 kg spacecraft to Mars (mission M1, scenario 27, capability = 5232 kg), but aerobraking would not (mission M1, scenario 26, capability = 4556 kg). The use of one Delta IV heavy vs two Delta IV mediums would result in a launch-vehicle cost savings of $48M, a result not represented in the methodology of Table 15. The original Centre National d'Etudes Spatiales plan for the 2005/2007 Mars sample return mission in fact proposed exactly this approach with the lander and the sample return orbiter launched on a single Ariane-5. A second important caveat for Mars is that if the time delay of multimonth aerobraking into orbit is not acceptable (e.g., if the orbiter must support landed assets immediately or if astronauts are onboard), then the aerocapture performance advantage in dollars/kilogram for the Mars M1 mission becomes much larger, increasing from 12 to 41% vs the next best option of advanced chemical (chem370) propulsive orbit insertion.

From a technology development point of view, it is desirable to estimate the total return on investment. Although aerocapture technology has considerable maturity, it is generally accepted that a flight-test experiment will be required before aerocapture will be used on any NASA science mission. Additionally, some level of modeling and ground-based experimentation will be required for the more challenging gas giant planet missions, particularly in the areas of aerothermodynamics and thermal protection systems. Based on the work in Refs. 8 and 11, it is estimated that the combination of flight test and gas giant planet development will require an investment on the order of $100M. According to the methodology used to generate Table 16, an investment of this magnitude will be returned in a single large V1, T1, or U1 mission, or two V2 missions. Alternatively, because aerocapture provides a factor of two or three increase in delivered mass for these missions at the same it can be argued that the science return is likewise doubled or tripled, thereby providing a two- or three-mission benefit for the price of one. At $300–$500M per mission, this equates to a manyfold return on the original $100M investment. Conversely, the investment return for M1 missions is not significant from the single-use-cost savings perspective, although the mass improvement shown in Table 15, and its associated increased science return, will eventually justify a $100M investment over the course of multiple missions.

By strict definition, aerocapture provides an infinite return on investment for the enabled missions to Jupiter, Saturn, and Neptune because there are no existing nonaerocapture alternatives that can

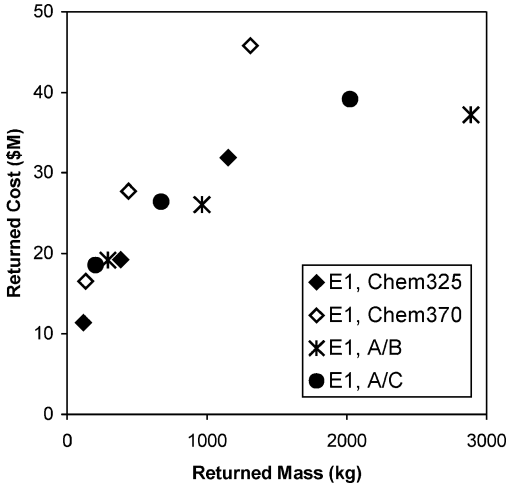

Fig. 5 Results from Earth mission E1

be used as reference points. However, it is important to note that an alternative enabling approach is being developed by NASA using nuclear electric propulsion (NEP) based on 100-kW-class fission reactors. In principle, this technology will be able to do the J1, S1, and N1 missions with the added benefits of abundant electrical power and propulsive capability once in orbit. However, there are no definitive estimates for the per unit cost of future NEP systems and so quantitative cost comparisons to aerocapture cannot be done at this time.

The last mission in the set is an aeroassisted orbit transfer from GTO to LEO at Earth (E1). As described earlier, this mission is of interest for three reasons: first, this is the likely implementation scenario for an Earth-orbit flight-test experiment of aerocapture; second, there are potential small spacecraft applications which require low Earth orbits even though secondary payload rides might only be available to GTO; and third, it is a reasonable proxy for future missions involving aeroassisted return of assets from the Lagrange points to low Earth orbit.

The methodology for analyzing mission E1 was different than the others because the assumed initial condition of a GTO orbit precludes consideration of the launch vehicle and in-space trajectory. Therefore, only steps 6 and 7 in Table 3 were involved in the computation. The results are shown in Fig. 5, where the size scaling is illustrated by simply computing arbitrary initial masses of 300, 1000, and 3000 kg. Not surprisingly, the aerobraking scenarios show a clear performance advantage at all scales. This results from the fact that aerobraking requires essentially no mass and, in this case, the usual precursor step of propulsive insertion into a high eccentricity orbit is not involved. The data also show that the operations cost of aerobraking is approximately the same as an aerocapture system, and so there is no net cost advantage either way. On a dollar/kilogram basis, aerocapture offers a 32% advantage vs conventional chemical ($I_{sp} = 325$ s) orbit insertion, whereas aerobraking offers a 54% advantage. However, although aerobraking is a clear winner on this basis, the need to make a large number of passes through the Van Allen radiation belts is likely to place unacceptable demands for radiation tolerance of the spacecraft and its cargo for most applications. For this reason, therefore, aerobraking at Earth will mostly be not attempted, leaving aerocapture as the preferred alternative to propulsive orbit transfer.

Conclusions

Aerocapture has been shown to provide enabling or substantially enhancing benefits to a large number of potential missions across the solar system compared to alternative orbit insertion techniques based on chemical propulsion, solar electric propulsion, and aerobraking. Delivery cost per unit delivered mass ($M/kg) has been the primary metric used to quantify aerocapture benefits, where the delivery cost includes all elements of the architecture from launch to orbit insertion. Of the 10 planetary missions in the defined set,

3 were found to be enabled by aerocapture (J1, S1, and N1), 5 were found to be enhanced (V1, V2, M1, T1, and U1), and 2 were not found to be helped (M2, J2). The normalized delivery costs based on a heavy-launch vehicle for the aerocapture-enabled or aerocapture-enhanced missions range from \$0.06M/kg for Mars orbiters (M1) to \$0.93M/kg for Saturn orbiters (S1). On a percentage basis, the \$M/kg cost reduction due to aerocapture ranges from 12% for the M1 mission to 100% reductions for the three enabled missions. The analysis shows that these results are not very sensitive to 30% increases in both the estimated aerocapture system mass and system cost. This suggests that even modestly performing aerocapture systems will yield substantial mission benefits. The detailed calculations show that aerocapture tends to increase the delivered spacecraft mass for approximately the same overall delivery cost on a given mission and launch vehicle. Substantial cost savings can nevertheless be achieved through use of aerocapture by switching to a smaller launch vehicle or by conducting greatly expanded science on a single mission vs two or more smaller and less capable nonaerocaptured missions. In particular, the projected cost savings on aerocapture-enhanced missions to Venus, Titan, and Uranus are sufficient to more than recoup the estimated \$100M cost for an Earth flight-test experiment. Aerocapture-enabled missions to Neptune, Saturn, and Jupiter are estimated to provide an infinite return on that investment, although the emergence of nuclear electric propulsion can serve as a finite comparative benchmark once definitive cost estimates for it become available. Finally, an Earth mission consisting of an aeroassisted orbit transfer vehicle going from geosynchronous transfer orbit to low Earth orbit showed that aerocapture offers a 32% \$/kg reduction compared to chemical propulsion. Aerobraking for this mission offers even better performance, but the problem of repeated passes through the Van Allen radiation belts are likely to preclude Earth aerobraking for most applications.

Acknowledgments

The authors acknowledge the trajectory analysis assistance of Carl Sauer, Jennie Johannesen, and Theresa Debban, all at Jet Propulsion Laboratory. The research described in this paper was performed at JPL, California Institute of Technology, under a contract with NASA and administered through the In Space Propulsion Program.

References

[1]Repic, E. M., Boobar, M. G., and Chapel, F. G., "Aerobraking as a Potential Planetary Capture Mode," *Journal of Spacecraft and Rockets*, Vol. 5, No. 8, 1968, pp. 921–926.

[2]Cruz, M. I., "The Aerocapture Vehicle Mission Design Concept," AIAA Paper 79-0893, May 1979.

[3]French, J. R., and Cruz, M. I., "Aerobraking and Aerocapture for Planetary Missions," *Astronautics and Aeronautics*, Vol. 18, Feb. 1980, pp. 48–55, 71.

[4]Walberg, G. D., "A Survey of Aeroassisted Orbit Transfer," *Journal of Spacecraft and Rockets*, Vol. 22, No. 1, 1985, pp. 3–18.

[5]Walberg, G. D., "Aerocapture for Manned Mars Missions—Status and Challenges," AIAA Paper 91-2870, Aug. 1991.

[6]Willcockson, W. H., "Mars Aerocapture Using Continuous Roll Techniques," AAS Paper 91-422, Aug. 1991.

[7]Wercinski, P. F., Henline, W., Tran, H., Milos, F., Papadopolous, P., Chen, Y.-K., and Venkatapathy, E., "Trajectory, Aerothermal Conditions and Thermal Protection System Mass for The Mars 2001 Aerocapture Mission," AIAA Paper 97-0472, Jan. 1997.

[8]Hall, J. L., "An Overview of the Aerocapture Flight Test Experiment (AFTE)," AIAA Paper 2002-4621, Aug. 2002.

[9]Rousseau, S., Perot, E., Graves, C., Masciarelli, J. P., and Queen, E., "Aerocapture Guidance Algorithm Comparison Campaign," AIAA Paper 2002-4822, Aug. 2002.

[10]Lockwood, M. K., "Titan Aerocapture Systems Analysis," AIAA Paper 2003-4799, July 2003.

[11]James, B., and Munk, M., "Aerocapture Technology Development Within the NASA In-Space Propulsion Program," AIAA Paper 2003-4654, July 2003.

[12]*New Frontiers in the Solar System: An Integrated Exploration Strategy*, Solar System Exploration Survey Committee, Space Studies Board, Div. of Engineering and Physical Sciences, National Research Council, National Academies Press, Washington, DC, 2003.

[13]"Solar System Exploration 2003," Jet Propulsion Lab., JPL 400-1077, NASA, May 2003, URL: http://spacescience.nasa.gov/admin/divisions/se/SSE_Roadmap.pdf.

[14]Rayman, M. D., "Results from the Deep Space 1 Technology Validation Mission," International Academy of Astronautics, Paper 99-IAA.11.2.01, Oct. 1999.

[15]Polk, J. E., Kakuda, R. Y., Anderson, J. R., Brophy, J. R., Rawlin, V. K., Patterson, M. J., Sovey, J., and Hamley, J., "In-Flight Performance of the NSTAR Ion Thruster Technology on the Deep Space One Mission," AIAA Paper 99-2274, June 1999.

[16]Christensen, J. A., Freick, K. J., Hamel, D. J., Hart, S. L., Norenberg, K. T., Haag, T. W., Patterson, M. J., Rawlin, V. K., and Sovey, J. S., "The NSTAR Ion Propulsion System for DS1," AIAA Paper 99-3372, June 1999.

[17]Patterson, M., Foster, J., Haag, T., Rawlin, V., Soulas, G., and Roman, R., "NEXT: NASA's Evolutionary Xenon Thruster," AIAA Paper 2002-3832, July 2002.

[18]Oleson, S., Gefert, L., Benson, S., Sims, J., Noca, M., and Patterson, M., "Mission Advantages of NEXT: NASA's Evolutionary Xenon Thruster," AIAA Paper 2002-3969, July 2002.

V. Zoby
Editor-in-Chief